

The High-Pressure Synthesis and Characterization of Some Praseodymium-Substituted Rare-Earth-Based $R_2\text{Ba}_4\text{Cu}_7\text{O}_{14+\delta}$ ($R = \text{Nd, Eu, Tm}$)

Teng-Ming Chen¹ and F. S. Kao

Department of Applied Chemistry, National Chiao-Tung University, Hsinchu 300, Taiwan, Republic of China

Received November 14, 1996; in revised form March 26, 1997; accepted April 2, 1997

The formation of phases in the $(R_{1-x}\text{Pr}_x)_2\text{Ba}_4\text{Cu}_7\text{O}_{14+\delta}$ (Pr-doped R247; $R = \text{Nd, Eu, Tm}$) system with $x = 0-1.0$ was investigated. Samples of the title series were synthesized at 980–990°C at 25 bar O_2 , followed by annealing at 300°C under 130 bar O_2 for 30 hr. Oxygen content of the samples has been determined by iodometric titration. Single-phased samples were obtained with x smaller than or equal to 0.3, 0.4, and 0.4 for $R = \text{Nd, Eu, and Tm}$, respectively, as indicated by X-ray diffraction measurements. With increasing amount of Pr substituting for R , the cell dimensions of the Pr-doped R247 phases were found to expand steadily, whereas the corresponding structural orthorhombicity was observed to decrease systematically. Superconducting transition temperatures (T_c 's) of the title phases were found to be significantly suppressed upon Pr doping, as indicated by field-cooled temperature-dependent magnetization studies. The effect of Pr substitution on T_c 's of R247 ($R = \text{Y, Eu, Er, Tm, Nd, Dy}$) phases was investigated and compared as a function of R^{3+} radii, but no size dependence effect was observed. In addition, field-dependent magnetization studies for a series of $(\text{Eu}_{1-x}\text{Pr}_x)_2\text{Ba}_4\text{Cu}_7\text{O}_{14+\delta}$ samples with $x = 0, 0.2, \text{ and } 0.4$, respectively, are also reported. © 1997 Academic Press

1. INTRODUCTION

The effect of Pr substitution for Y on the structural and superconducting properties of the $n = 0$ (1–3), $n = 1$ (4–6), and $n = 2$ (7–10) members of the $\text{Y}_2\text{Ba}_4\text{Cu}_{6+n}\text{O}_{14+n-\delta}$ homologous series has been extensively investigated and superconductivity in these cuprates has been found to be dramatically suppressed, in contrast to the similar substitution by other rare earths. However, there have been few investigations of Pr substitution in the $R_2\text{Ba}_4\text{Cu}_7\text{O}_{14+\delta}$ phases (R247, $R = \text{rare earths}$) reported in the literature except those (i.e., Pr-substituted Er247 and Dy247 phases) studied by Tarntair (11). The formation of Pr-doped R247

phases provides us an opportunity to probe the phenomenon of superconducting transition temperature (T_c) depression upon Pr doping and to understand possible correlations between magnetic properties and high-temperature superconductivity in the Pr-doped R247 phases. We have previously investigated and reported elsewhere several series of $(R_{1-x}\text{Pr}_x)_2\text{Ba}_4\text{Cu}_7\text{O}_{14+\delta}$ phases with $R = \text{Y, Sm, Gd, Dy, Ho, and Er}$, respectively (4, 11, 12). In this paper we describe the synthesis, oxygen compositions, and structural and physical properties of three series of Pr-doped R247 phases with $R = \text{Nd, Eu, and Tm}$. In particular, we have examined the effect of Pr substitution for R , variation of oxygen compositions, and the size of R^{3+} ions on the superconductivity of the title R247 phases.

2. EXPERIMENTAL

Samples of $(R_{1-x}\text{Pr}_x)_2\text{Ba}_4\text{Cu}_7\text{O}_{14+\delta}$ series with $R = \text{Nd, Eu, and Tm}$, respectively, were prepared following the procedures described in the previous paper by Kao and Chen (13). Briefly, the Pr-doped R247 phases were prepared by prereacting a stoichiometric mixture of $R_2\text{O}_3$ ($R = \text{Nd, Eu, Tm}$), $\text{Ba}(\text{NO}_3)_2$, CuO , and Pr_6O_{11} in alumina crucibles at 900–920°C under flowing oxygen gas with several intermittent grindings to maximize homogeneity. The reacted mixture was then removed from the furnace and quenched to room temperature, and then it was wrapped in gold foil and rereacted at 980–990°C for 24 hr in an atmosphere of 25 bar of oxygen, followed by a 30-hr annealing at 300–320°C under 120–130 bar of oxygen by using a commercially available high-pressure oxygen system (Model HPS-3210P, Morris Research Co., U.S.A.). The high-pressure furnace is externally heated and equipped with a generous sample space (e.g., 10 mm in diameter and 50 mm in length) and a safety relief valve to assure safe operations. Oxygen content of the samples has been determined by a modified iodometric titration technique previously described by Appelmann *et al.* (14).

¹To whom correspondence should be addressed.

The X-ray diffraction (XRD) data ($5^\circ \leq 2\theta \leq 70^\circ$, step-width 0.02°) of samples were obtained using graphite-monochromatized $\text{CuK}\alpha$ radiation from an automatic powder diffractometer (Model MXP-3, MAC Science Co., Japan) equipped with a Ni filter. The field-cooled dc magnetic susceptibility of powder samples of Pr-doped R247 as a function of temperature was measured with a SQUID magnetometer (Model MPMS5, Quantum Design Co., U.S.A.) over the temperature range of 100–5 K in a magnetic field strength of 15 Gauss. The magnetization hysteresis curves for a series of $(\text{Eu}_{1-x}\text{Pr}_x)_2\text{Ba}_4\text{Cu}_7\text{O}_{14+\delta}$ samples with $x = 0, 0.2$, and 0.4 were obtained at 5 K in an applied field from 0 to 6 Tesla. The X-ray photoelectron spectra (XPS) of $(\text{R}_{0.8}\text{Pr}_{0.2})_2\text{Ba}_4\text{Cu}_7\text{O}_{14+\delta}$ ($R = \text{Nd}$ and Eu) samples were measured on a Perkin-Elmer PHI 590 AM spectrometer using monochromatized $\text{AlK}\alpha_{1,2}$ ($h\nu = 1486.6$ eV) X-ray incident radiation, with the analyzer resolution set at nominal value of 0.4 eV. The as-prepared samples were introduced into the spectrometer chamber without further surface cleaning or sputtering to avoid changes in oxygen composition.

3. RESULTS AND DISCUSSION

Samples of the $(\text{R}_{1-x}\text{Pr}_x)_2\text{Ba}_4\text{Cu}_7\text{O}_{14+\delta}$ phases with $x = 0.3, 0.4$, and 0.4 were single phased and the limits of substitution were also determined to be 0.3–0.4, 0.4–0.5, and 0.4–0.5 in x for $R = \text{Nd}$, Eu , and Tm , respectively, as

indicated by the measured XRD data. Both the pristine and the Pr-doped R247 phases appear to exist in a relatively narrow range of pressure (i.e., 20–35 bar of oxygen), whereas their stability is less sensitive to temperature variation. The range of stability of R247 phases was found to be comparable to that reported by Karpinski *et al.* (15) (i.e., $8 \leq P \leq 2900$ bar O_2 and $860^\circ\text{C} \leq T \leq 1100^\circ\text{C}$) and that reported by Morris *et al.* (16) (i.e., $10 \leq P \leq 30$ bar O_2 and $930^\circ\text{C} \leq T \leq 980^\circ\text{C}$), respectively, for $\text{Y}_2\text{Ba}_4\text{Cu}_7\text{O}_{15-x}$ phase. The lattice parameters a , b , c , and unit cell volume (vol.) of the Pr-doped R247 phases, determined from the XRD data by a least-square refinement method, are represented as a function of Pr content (x) and summarized in Fig. 1. The cell dimensions of all three series of Pr-doped R247 phases were found to expand monotonically with increasing Pr contents. This observation may be attributed to the fact that the ionic radius of eight-coordinated Pr^{3+} is relatively larger than that of any of the following eight-coordinated R^{3+} ions, i.e., Pr^{4+} (0.96 Å) < Tm^{3+} (0.99 Å) < Er^{3+} (1.00 Å) < Y^{3+} (1.02 Å) < Eu^{3+} (1.07 Å) < Nd^{3+} (1.12 Å) < Pr^{3+} (1.14 Å) (17). An opposite trend of cell dimensions variation would have been observed if the Pr ion were present in a valence state of 4+. Furthermore, as summarized in Fig. 2, the orthorhombicity, $2(b-a)/(b+a)$, of unit cell of Pr-doped phases was found to decrease with increasing Pr content for all of the three Pr-doped R247 phases investigated. This observation indicates that the structural anisotropy of the title Pr-doped R247 phases

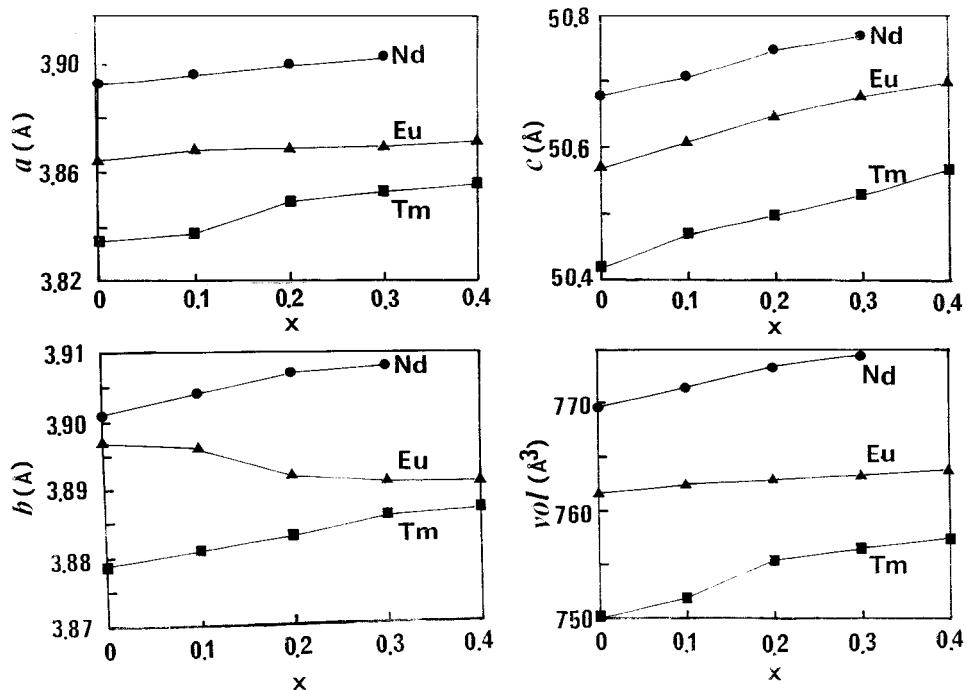


FIG. 1. The lattice parameters a , b , c , and vol. of Pr-doped R247 phases with $R = \text{Nd}$, Eu , and Tm as a function of Pr content (x).

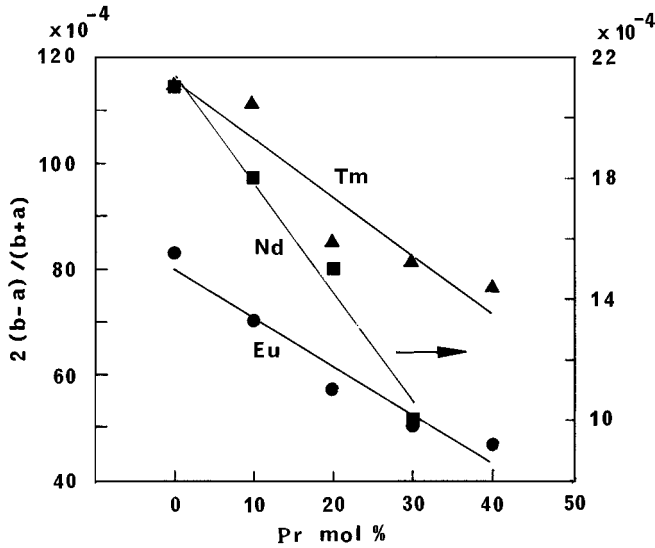


FIG. 2. The structural orthorhombicity as a function of Pr content (x) for Pr-doped R247 samples with $R = \text{Nd}$ (■), Eu (●), and Tm (▲), respectively.

becomes less upon Pr substitution, which may presumably be attributed to the stronger extent of hybridization of Pr 4*f* and oxygen 2*p* orbitals, compared to those of systems with other rare-earth atoms. The same trend of orthorhombicity reduction with increasing Pr content has also been observed in other Pr-doped R247 series with $R = \text{Y, Gd, Sm, Ho, Er,}$ and Dy , respectively (11, 12).

The T_c 's of the three Pr-doped R247 series, as determined by field-cooled (15 Gauss) temperature-dependent magnetic susceptibility measurements, are presented in Fig. 3 and simultaneously summarized in Table 1. T_c 's of the $(R_{1-x}\text{Pr}_x)_2\text{Ba}_4\text{Cu}_7\text{O}_{14+\delta}$ phases were found to drop significantly upon Pr substitution from 66, 75, and 88 K down to 41, 52, and 50 K as x increases from 0 to 0.3, 0.4, and 0.4 for $R = \text{Nd, Eu,}$ and Tm , respectively. Also shown in Table 1 are the oxygen contents ($14 + \delta$) of Pr-doped R247 samples and the ranges of composition distribution are 14.525–14.603 for Nd series, 14.632–14.788 for Eu series, and 14.525–14.732 for Tm series, respectively, as determined by iodometric titration. In general, the oxygen compositions of the Pr-doped samples tend to vary slightly or decrease as the Pr content increases. The scattered distribution of oxygen content in different samples may most likely be attributed to the difference in preparation conditions in spite of our effort to keep them constant during sample preparations. However, we do not rule out the possibility that oxygen composition in different Pr-doped R247 samples may be strongly dependent on and vary systematically with the Pr dopant content.

To further understand the effect and extent of Pr-doping on T_c of the R247 phases, the dopant-composition (x) coefficient

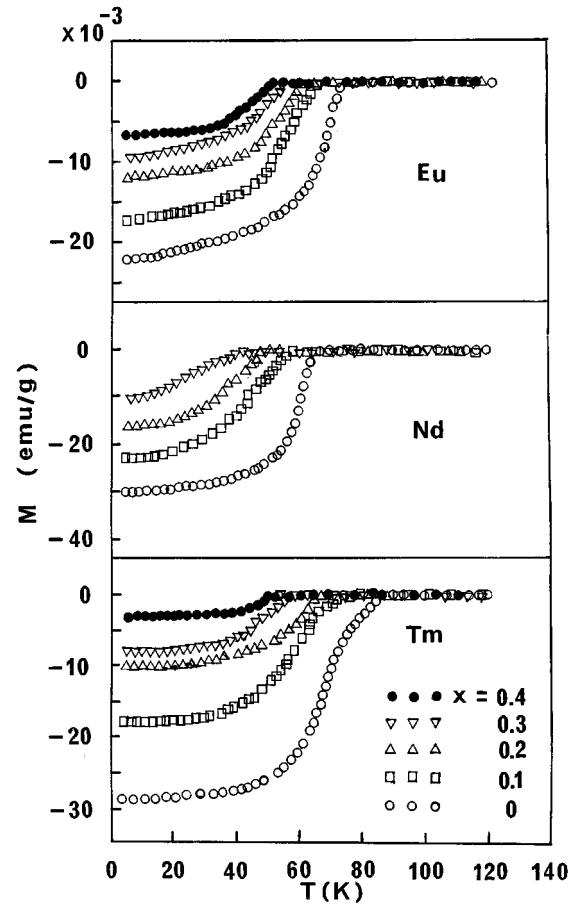


FIG. 3. The T_c as a function of Pr content (x) for Pr-doped R247 samples with $R = \text{Nd, Eu,}$ and Tm , respectively, as determined from Meissner effect.

icients of T_c (i.e. $|dT_c/dx|$) for the title phases were determined to be 41.7, 28.8, and 47.5 K/Pr atom per formula unit (f.u.) for Pr-doped R247 phases with $R = \text{Nd, Eu,}$ and Tm , respectively. These results together with those obtained in

TABLE 1
The Transition Temperature, T_c (Determined from Meissner Effect), and Oxygen Contents ($14 + \delta$) for $(R_{1-x}\text{Pr}_x)_2\text{Ba}_4\text{Cu}_7\text{O}_{14+\delta}$ ($R = \text{Nd, Eu, Tm}$) Phases

| $x =$ | 0 | 0.1 | 0.2 | 0.3 | 0.4 |
|-----------------|-------|-------|-------|-------|-------|
| $R = \text{Nd}$ | | | | | |
| T_c | 66 | 56 | 48 | 41 | — |
| δ | 0.525 | 0.587 | 0.603 | 0.541 | — |
| $R = \text{Eu}$ | | | | | |
| T_c | 75 | 68 | 63 | 58 | 52 |
| δ | 0.671 | 0.779 | 0.761 | 0.632 | 0.788 |
| $R = \text{Tm}$ | | | | | |
| T_c | 88 | 76 | 68 | 60 | 50 |
| δ | 0.732 | 0.725 | 0.722 | 0.667 | 0.652 |

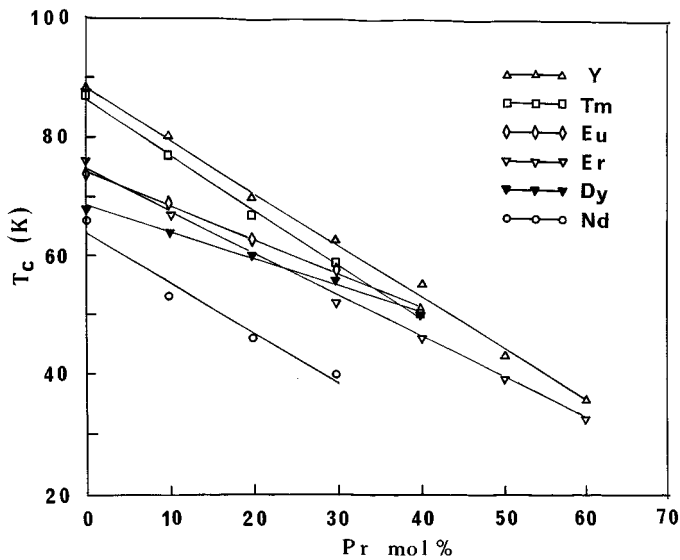


FIG. 4. The T_c dependence of Pr dopant composition in Pr-doped R247 ($R = Y, Nd, Tm, Eu, Er, Dy$) phases showing that the magnitude of $|dT_c/dx|$ for $R = Tm$ is the largest and that for Dy is the smallest.

other $(R_{1-x}Pr_x)_2Ba_4Cu_7O_{14+\delta}$ ($R = Y, Dy, Er$) series reported previously by our group (11,12) are summarized in Fig. 4. The magnitude of $|dT_c/dx|$ for the series with $R = Tm$ was found to be the greatest, whereas that (i.e., 22.0 K/Pr atom per f.u.) for those with $R = Dy$ is the smallest. We therefore did not observe any R^{3+} size dependence of the $|dT_c/dx|$ value in this investigation, as might have been expected for a series of Pr-doped R247 phases with different R 's. Our observations could probably be attributed to the difference in oxygen stoichiometry of the Pr-doped R247 samples.

To investigate the effect of Pr doping on the flux pinning in the R247 phases, the magnetic hysteresis $M-H$ loops of three $(Eu_{1-x}Pr_x)_2Ba_4Cu_7O_{14+\delta}$ ($x = 0, 0.2, 0.4$) samples were measured at 5 K by using a dc SQUID magnetometer, respectively, and the results are shown in Fig. 5. The shape of M/H loops was found to be similar to that of the $(Er_{0.5}Pr_{0.5})_2Ba_4Cu_7O_{14+\delta}$ (11) which also contains magnetic Er^{3+} ion and the area of the $M-H$ loops of the Pr-doped Eu247 phases was observed to become gradually reduced with increasing Pr concentration. The effect of magnetic moment and the amount of Pr^{3+} and Eu^{3+} ions on the variation of area of field-dependent magnetization loops of the Pr-doped Eu247 samples are currently under investigations.

The core-level XPS spectra of Cu $2p_{3/2}$ for samples of $(R_{0.8}Pr_{0.2})_2Ba_4Cu_7O_{14+\delta}$ ($R = Nd$ and Eu) were measured and shown in Figs. 6a and 6b, respectively. An attempt was made to deduce the correlation between empirically derived atomic ratios of Cu^{2+}/Cu^{3+} obtained by different methods

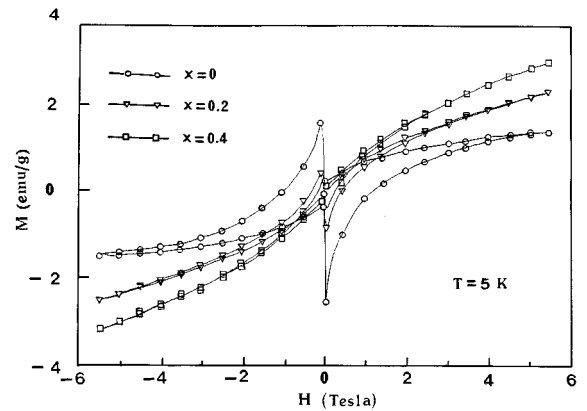


FIG. 5. The magnet hysteresis curves for $(Eu_{1-x}Pr_x)_2Ba_4Cu_7O_{14+\delta}$ samples as a function of Pr composition for $x = 0, 0.2,$ and 0.4 at 5 K, respectively.

(i.e., XPS spectrometry and iodometric titration). The presence of Cu^+ species was ruled out under the preparative conditions of high oxygen pressure when the XPS spectra were analyzed. Therefore, the peaks assigned to Cu atoms were assumed to be contributed from Cu^{3+} and Cu^{2+} ions

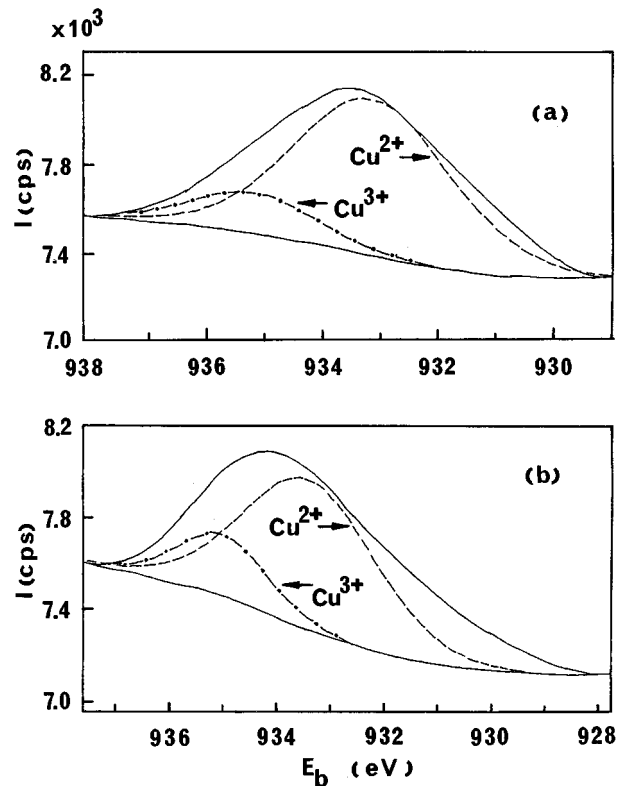


FIG. 6. The core-level XPS spectra of Cu $3p_{3/2}$ for $(R_{0.8}Pr_{0.2})_2Ba_4Cu_7O_{14+\delta}$ samples with $R = (a)$ Nd and (b) Eu, respectively.

TABLE 2

Comparison of E_b , Integrated Areas (A) of Deconvoluted Cu^{2+} and $\text{Cu}^{3+}2p_{3/2}$ Peaks, Oxygen Contents ($14+\delta$) and the Discrepancy in Oxygen Content ($\Delta\delta$) for $(R_{0.8}\text{Pr}_{0.2})_2\text{Ba}_4\text{Cu}_7\text{O}_{14+\delta}$ ($R = \text{Eu, Nd}$) Samples Determined from XPS Deconvolution and Iodometric Titration, Respectively

| R | $E_b(\text{Cu}^{3+})$ (eV) | $E_b(\text{Cu}^{2+})$ (eV) | $A(\text{Cu}^{3+})^a$ | $A(\text{Cu}^{2+})^a$ | $A(\text{Cu}^{2+})/A(\text{Cu}^{3+})$ | δ^b | δ^c | $\Delta\delta$ |
|-----|----------------------------|----------------------------|-----------------------|-----------------------|---------------------------------------|------------|------------|----------------|
| Nd | 935.20 | 933.20 | 46.5 | 231.5 | 4.978 | 0.585 | 0.603 | 3.0% |
| Eu | 935.00 | 933.40 | 55.9 | 203.5 | 3.640 | 0.754 | 0.761 | 1.0% |

^aIn arbitrary units.

^bOxygen content determined from XPS peak deconvolution.

^cOxygen content determined from iodometric titration.

with binding energy (E_b) centered at 935 and 933.5 eV, respectively (18). The Cu $2p_{3/2}$ peaks of the measured spectra were then deconvoluted into two components centered at 935.20 and 933.20 eV in E_b 's for samples containing Nd and those at 935.00 and 933.40 eV for samples containing Eu, respectively, according to the methods described by Cohen *et al.* (18) and Karlsson and Gunnarsson (19). Summarized in Table 2 are the relative atomic ratios of $\text{Cu}^{2+}/\text{Cu}^{3+}$ for both samples, as estimated by integrating the areas of deconvoluted peaks corresponding to Cu^{2+} and Cu^{3+} ions, $A(\text{Cu}^{2+})$ and $A(\text{Cu}^{3+})$, in the spectra shown in Figs. 6a and 6b, respectively. The oxygen contents ($14 + \delta$) derived from the $A(\text{Cu}^{2+})/A(\text{Cu}^{3+})$ ratio are also reported in Table 2. Regardless of different samples, there appears to be a very good agreement (i.e., deviation of 2–3%) on oxygen contents between those derived from XPS spectra and those determined by iodometric titrations on the two samples, as indicated in Table 2.

4. CONCLUSIONS

Three series of rare-earth-based R247 cuprates with the title compositions have been synthesized using high-pressure techniques. The substitution limit of Pr for R was determined to be 30–40%, 40–50%, and 40–50% for $R = \text{Nd, Eu, and Tm}$, respectively. As the dopant content increases, T_c 's of Pr-doped R247 phases were found to decrease, whereas the cell dimensions were found to increase monotonically. Furthermore, T_c 's were found to drop from 66, 75, and 88 K down to 41, 52, and 50 K as x increases from 0 to 0.3, 0.4, and 0.4 for $R = \text{Nd, Eu, and Tm}$, respectively. The coefficients of $|dT_c/dx|$ were found to be 41.7, 28.8, and 47.5 K/Pr atom per formula unit for Pr-doped R247 samples with $R = \text{Nd, Eu, and Tm}$, respectively, indicating the absence of R^{3+} ion size dependence. The flux pinning in Pr-doped R247 phases was found to be enhanced with increasing doped Pr content, as indicated by Pr composition-dependent magnetic M/H loop measurements. The oxygen contents of the title Pr-doped R247 phases determined by iodometric titration were in good agreement with those derived from XPS spectrometry.

ACKNOWLEDGMENTS

We thank the National Science Council of the Republic of China for financial support through Grants NSC81-0204-M-009-02 (high-pressure furnace) and NSC84-2113-M-009-013. The magnetic measurements were carried out at the Regional Instruments Centers of NSC located in Hsinchu and Tainan, respectively. We also thank Prof. H-C. I. Kao of Tamkang University for assistance with the iodometric titration analyses.

REFERENCES

1. L. Solderholm, K. Zhang, D. G. Hinks, M. A. Beno, J. D. Jorgenson, C. U. Segre, and I. K. Schuller, *Nature* **328**, 604 (1987).
2. J. L. Peng, P. Klavins, R. N. Shelton, H. B. Radousky, P. A. Hahn, and L. Bernardez, *Phys. Rev. B* **40**, 4517 (1989).
3. J. K. Liang, X. T. Xu, S. S. Xie, G. H. Rao, X. Y. Shao, and Z. G. Duan, *Z. Phys. B* **69**, 137 (1987).
4. F.-G. Tarntair and T.-M. Chen, *Phys. C* **235–240**, 367 (1994).
5. N. Seiji, S. Adachi, and H. Yamaguchi, *Phys. C* **235–240**, 365 (1994).
6. A. Matsushita, T. Yamanishi, Y. Yamada, N. Yamada, S. Takashima, S. Hiroi, K. Kawamoto, I. Hirabayashi, Y. Kodama, M. Otsuka, and T. Matsumoto, *Phys. C* **227**, 254 (1994).
7. S. Adachi, N. Watanabe, N. Seiji, N. Koshizuka, and H. Yamauchi, *Phys. C* **207**, 127 (1993).
8. J. Herrmann, U. C. Boehnke, M. Krotzsch, B. Lippold, and F. Schlenkerich, *Phys. C* **221**, 76 (1994).
9. H. B. Liu, D. E. Morris, A. P. B. Sinha, and G. H. Kwei, *Phys. C* **223**, 51 (1994).
10. Z. Gou, N. Yamada, K. I. Gondaira, T. Iri and K. Kohn, *Phys. C* **220**, 41 (1994).
11. F. G. Tarntair, M.S. Thesis, National Chiao Tung University, Taiwan, (1994).
12. T.-M. Chen, Y. L. Lai, and F. S. Kao, *Phys. C*, in press (1997).
13. F.-S. Kao and T.-M. Chen, *Chin. J. Phys. (Taipei)* **34**(2), 561 (1996).
14. H. Appelman, L. E. Moress, A. M. Kini, U. Geiser, A. Umezawa, G. W. Crabtree, and K. D. Carlson, *Inorg. Chem.* **26**, 3237 (1987).
15. J. Karpinski, S. Rusiecki, B. Bucher, E. Kaldis, and E. Jilek, *Phys. C* **161**, 618 (1989).
16. D. E. Morris, N. G. Asmar, J. H. Nickel, R. L. Sid, and J. Y. T. Wei, *Phys. C* **159**, 287 (1989).
17. R. D. Shannon and C. T. Prewitt, *Acta. Crystallogr. B* **25**, 925 (1969).
18. O. Cohen, F. H. Potter, C. S. Rastomjee, and R. G. Egdell, *Phys. C* **201**, 58 (1991).
19. K. Karlsson and D. Gunnarsson, *J. Phys. Condens. Matt.* **4**, 2801 (1992); K. Karlsson and D. Gunnarsson, *J. Phys. Condens. Matt.* **4**, 895 (1992).